

STRUCTURAL AND MAGNETIC PROPERTIES OF $\text{SrM}_{0.5}\text{Fe}_{11.5}\text{O}_{19}$ (M: Ti^{4+} , Co^{2+} , Ni^{2+} , Cu^{2+} , AND Zn^{2+}) DERIVED FROM STEEL WASTE PRODUCT VIA MECHANICAL ALLOYING

N.Daud*, R.S.Azis^{1,2}, M. Hashim², K.A. Matori^{1,2}, N.M.M.Shahrani², S.Sulaiman², N.N.C.Muda², A. H. Azizan¹, M. A. Musa¹

¹Department of Physics, Universiti Putra Malaysia, 43400 UPM Serdang, Selangor, Malaysia

²Institute of Advanced Technology, Universiti Putra Malaysia, 43400 UPM Serdang, Selangor, Malaysia

ABSTRACT

This paper presents the steel waste product used as the main source of raw material in the preparation of permanent magnets ferrites, substitution with transition metal cation. M-type hexaferrites of $\text{SrM}_{0.5}\text{Fe}_{11.5}\text{O}_{19}$ (M: Ti, Co, Ni, Cu, and Zn) component were investigated. Samples were prepared by Mechanical Alloying (MA) process and analysis microstructure of samples were characterized by using X-ray Diffraction (XRD). The specific saturation magnetization M_s , the coercivity H_c and remanence M_r was carried out using B–H hysteresis measurement. The XRD patterns show single phase of the magnetoplumbite strontium ferrite and Fe_2O_3 phases were only present in Ti^{4+} substitution. Significant increase in calculated lattice parameter a , c and cell volume V_{cell} from XRD indicating solubility of substituted cation in hexagonal structure of strontium ferrite. Magnetization measurements discovered that saturation magnetization M_s of the all samples proportional to magnetic moment μ_B of substituted cation with highest 28.33 emu/g from Co^{2+} . While highest coercivity 26.5 kA/m from Co^{2+} and for remanence Zn^{2+} 0.955 Tesla. The magnetic properties such as remanence B_r and coercivity H_c make the synthesized materials useful for high density recording media and permanent magnets.

Strontium ferrite is used in permanent magnets market because of their low price combined with reasonable magnetic performances [1]. Ceramic ferromagnetic materials mainly compose of iron (III) oxide, which is called ferrites. Ferrite magnets are known as ceramic magnets because of their fabrication method and electrical insulation characteristics [2]. Due to this reason, ferrites are used in high-frequency circuits as magnetic cores. Besides that, it is also known as ferrite permanent magnets or more specifically, should be acknowledged as hexagonal ferrite permanent magnet. The hexagonal ferrite structure can be found in both strontium hexaferrite, $\text{SrFe}_{12}\text{O}_{19}$, and barium hexaferrite, $\text{BaFe}_{12}\text{O}_{19}$. The raw material used to form ferrite magnet is strontium carbonate and iron oxide which are low in cost and readily available. In recent years, magnetic materials such as hexagonal ferrites $\text{SrFe}_{12}\text{O}_{19}$ have involved considerable attentions. They are extensively studied for their potential applications in microwave devices [3], high-density magnetic recording [4], electronic devices and medicine. Several cations has been used for substitution on the M-type hexaferrites, such as Ti^{3+} , Cr^{3+} , Pb^{3+} , La^{3+} , Gd^{3+} , Er^{3+} , and Ce^{3+} , which have been investigated and discussed [5, 6]. In this study we find that substitutions profoundly affect the structural and magnetic properties of the strontium hexaferrite system. The effect of (M: Ti, Co, Ni, Cu, and Zn) on its structure, magnetic properties and density will be discussed.

The mill scales were first crushed for several hours, then the powder underwent the Impurities Separation (IMS) Technique where the powder was placed in a glass tube with applies of 1 Tesla external magnetic field. The steel scrap was then carried out for Curie Temperature Separation Technique (CTST) procedure. The Fe_2O_3 is used from processes mill scales and appropriate amounts of high purity SrCO_3 , ZnO , CuO , CoO , NiO and TiO_2 powders were weighed and mixed to prepare $\text{SrM}_{0.5}\text{Fe}_{11.5}\text{O}_{19}$ by high energy ball mill (HEBM) using a SPEX800D HEBM machine at room temperature. The powder mixture is then pre-sinter at 950 °C for 10 hours by using the carbolite furnace, and then added with Polyvinyl Alcohol solution for granulation. The powder was then pressed at 300 MPa to a rod with the dimension of 10.5 mm × 8 mm radius and length. The samples were sintered in an ambient air condition at a temperature of 1200 °C for 10 hours in furnace. The structural properties and phase fractions were investigated using an X-ray powder diffractometer Philips X'pert Diffractometer model 7602 EA Almelo. The magnetic measurement was carried out using vibrating sample magnetometer (VSM) (model Lakeshore, 7404 series) at room temperature. The B–H hysteresis curves of the samples were obtained by measuring the impedance of a coil wound around the cylinder samples, with a soft magnetic materials automatic test system (MATS- 3010s) at

room temperature under an applied magnetic field of 4000 A/m (~ 50 Oe). Characteristic lattice parameters a and c for all the samples were calculated according to the formula 2 [7]:

$$\frac{1}{d^2} = \frac{4}{3} \left(\frac{h^2 + hk + k^2}{a^2} \right) + \frac{l^2}{c^2} \quad (1)$$

Where d is the inter-planer spacing calculated by Bragg formula ($2d \sin \theta = \lambda$), while $(h k l)$ are the Miller indices. The crystalline size (D) was obtained by using Scherrer formula, and tabulated in Table 1.

X-ray diffraction analysis. Figure 1 shows the X-ray diffraction patterns of the $\text{SrM}_{0.5}\text{Fe}_{11.5}\text{O}_{19}$ (M: Ti, Co, Ni, Cu, and Zn) M-type hexaferrite samples. All patterns were indexed and observed the inter-planer spacing d values of all the peaks and compared with the standard pattern for hexagonal strontium ferrite ICSD reference code (01-079-1411) space group P63/mmc with calculated density 5.14 g/cm³ [8]. The analysis of observed patterns shows that all peaks are related to the pure M-type hexagonal phase and extra peak is Fe_2O_3 observed at cation Ti^{4+} with ICSD reference code (01-089-0599). The peaks of substituted ferrites appear at the same positions with different intensities and full width at half maximum (FWHM). Table 1 show lattice parameter a of cation substituted compounds is larger than that of pure Strontium hexaferrite [9], This expansion can be attributed to larger ionic radii for Ti (0.0605 nm), Co (0.0745 nm), Ni(0.069 nm), Cu(0.073 nm) and Zn (0.074 nm), as compared to the ionic radius of Fe that is 0.055 nm [10]. The unit cell volume inversely proportional with X-ray density in all samples which is smaller than standard strontium hexaferrite 686.43 pm³. The unit cell volume was calculated with the lattice parameters a and c by the formula [7]:

$$V_{cell} = \frac{\sqrt{3}}{2} a^2 c \quad (2)$$

The X-ray density (ρ_x) was calculated according to the relation [7]:

$$\rho_x = \frac{2M}{N_a V_{cell}} \quad (3)$$

Where the constant number ‘2’ denotes the number of formula units in a unit cell, M represents the molar mass of the sample, and N_a is the Avogadro’s number. The values of lattice parameters, unit cell volumes and X-ray density are given in Table 1. The average crystallite size (D) of the synthesized samples was calculated from the Scherer formula [11].

$$D = \frac{k\lambda}{\beta \cos \theta} \quad (4)$$

Where k is the X-ray wavelength, β is the half peak width, θ is the Bragg angle and the value of shape factor $k = 0.89$ for hexaferrites [11]. The average crystallite size (D) was calculated from the width of the most intense peak and was found to be in the range of 55-75 nm (Table 1).

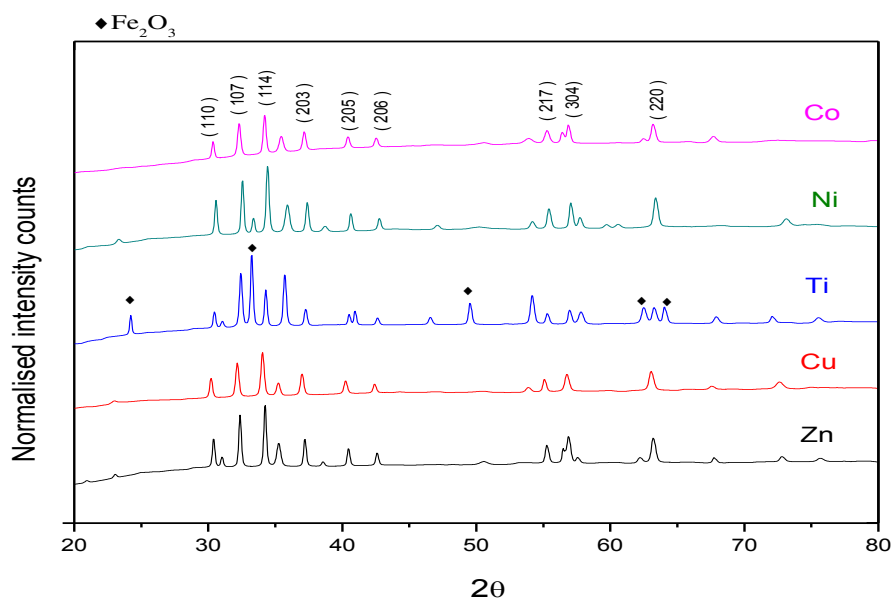


Figure 1: XRD patterns of $\text{SrM}_{0.5}\text{Fe}_{11.5}\text{O}_{19}$ cation substituted samples.

Table 1: Summary of powder X-ray diffraction measurements and crystallite size for difference cation substitution samples.

Cation	$2\theta(^{\circ})$		d -Value (\AA)		FWHM ($^{\circ}$)	Miller Indices	Lattice Constant		ρ_x (gcm^{-3})	V_{cell} (pm^3)	Crystallite size D (nm)
	Standard	Observed	Standard	Calculated			$a(\text{\AA})$	$c(\text{\AA})$			
Cu^{2+}	32.45	32.12	2.75	2.78	0.25	(107)	5.93	23.22	5.00	708.2	54.9
	34.26	34.01	2.61	2.63	0.26	(114)					55.2
Co^{2+}	32.45	32.28	2.75	2.77	0.26	(107)	5.89	23.12	5.07	695.9	54.9
	34.26	34.18	2.61	2.62	0.22	(114)					63.2
Zn^{2+}	32.45	32.35	2.75	2.76	0.16	(107)	5.88	23.06	5.11	692.2	87.9
	34.26	34.21	2.61	2.62	0.19	(114)					73.7
Ti^{4+}	32.45	32.40	2.75	2.76	0.22	(107)	5.87	23.03	5.10	688.4	62.9
	34.26	34.26	2.61	2.61	0.19	(114)					73.6
Ni^{2+}	32.45	32.53	2.75	2.75	0.19	(107)	5.85	22.94	5.18	680.9	73.3
	34.26	34.40	2.61	2.62	0.22	(114)					63.2

Magnetic characterization. Figure 2 (a)-(b) show the relationship of magnetic moment of cation and saturation magnetization and coercivity relate with crystalline size of M-type hexaferrite $\text{SrM}_{0.5}\text{Fe}_{11.5}\text{O}_{19}$. Each Fe^{3+} ion has five unpaired electrons, the total 12Fe^{3+} ions are distributed at five different sub-lattices in the M-type hexaferrites, three octahedral ($12k$, $2a$, $4f_2$), one tetrahedral ($4f_1$) and one is trigonal bipyramidal ($2b$). Out of 12Fe^{3+} ions four have the spin in downward direction that is at $4f_1$ (2Fe^{3+}) and $4f_2$ (2Fe^{3+}) while other 8Fe^{3+} ions have the spin in upward direction that is at $12k$ (6Fe^{3+}), $2a$ (1Fe^{3+}) and $2b$ (1Fe^{3+}). The four upward and four downward spin cancel each other and the net magnetic moment is only due to the remaining four iron ions having spin in the upward direction. The magnetic properties of the substituted hexaferrites strongly depend upon the electronic configuration of the substituting cations. It is well known, that more electronegative ions preferentially occupy octahedral coordination [12, 13].

It was reported that Co^{2+} and Cu^{2+} ions occupy on the tetrahedral $4f_1$ and octahedral $4f_2$ positions. The cation Co^{2+} and Cu^{2+} occupies the $4f_2$ (octahedral site) which is a low spin state contributing negatively to the total saturation

magnetization [14]. On the other substitution Ni^{2+} , Zn^{2+} , and Ti^{4+} ions replace Fe^{3+} ions at $4f_2$ and $12k$ sites for small values of substitution and prefers $12k$ site for larger amounts [13, 15]. Figure 2(a) show the relationship of moment with saturation magnetization is proportionally, some of Ni^{2+} ions with magnetic moment of $2 \mu_B$ are replaced with Fe^{3+} ions having magnetization of $5 \mu_B$ at $12k$ in high spin state, which is a result in decrease of M_s . For Zn and Ti cation, M_s decreases due to the presence of non-magnetic ions in the crystal structure, which decreases the exchange interactions between the Fe^{3+} ions. The radius of Fe^{3+} ions at octahedral site is 0.67 \AA and that of Cu^{2+} is 0.78 \AA . After the substitution, the c-axis length increases slightly which decrease the effect of low spin state contributions ($4f_1$ and $4f_2$) to magnetization (Table 1). As a result, like other cation substitution saturation magnetization is slightly less than that of the pure strontium hexaferrite which depending on preparation conditions [10, 16].

Figure 2 (b) show the coercivity is an extrinsic property, which depends upon the microstructure and may be enhanced by controlling the crystalline size, shape and size distribution [17]. It is also reported that the ferrite materials having low coercivity and high in remanence are suitable for magnetic recording applications such as in hard disks, floppy disks, video tapes, etc. [18]. This properties show by Ni^{2+} substitution with lower coercivity but high in remanence.

Table 2: Magnetic parameters of the $\text{SrM}_{0.5}\text{Fe}_{11.5}\text{O}_{19}$ samples, magnetic moments and ionic radiuses of the substituted cations.

Cation	Magnetic moment, μ_B	Ionic Radii, \AA	Coercivity, H_c (kA/m)	Remanence, B_r (T)	M_s (emu/g)
Cu^{2+}	1	0.730	26.5	0.0873	8.25
Co^{2+}	3	0.745	24.0	0.0839	28.33
Zn^{2+}	0	0.740	22.3	0.0955	6.75
Ti^{4+}	1	0.605	15.2	0.0714	11.4
Ni^{2+}	2	0.690	5.1	0.0727	20.93

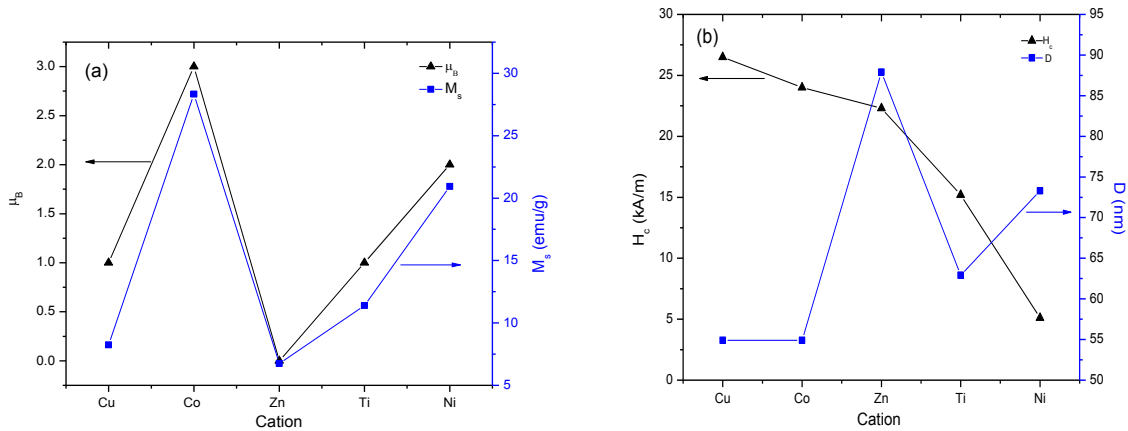


Figure 2: (a) The cation moment versus saturation magnetization of $\text{SrM}_{0.5}\text{Fe}_{11.5}\text{O}_{19}$, (b) the coercivity versus crystallite size.

A simple and economical method was used for synthesis of $\text{SrM}_{0.5}\text{Fe}_{11.5}\text{O}_{19}$ (M: Ti, Co, Ni, Cu, and Zn) by HEBM technique. The XRD analysis shows the lattice parameter (a) and (c) expansion. It shows that the value of the coercivity H_c is higher for Cu^{2+} 26.5 kA/m. However, the maximum saturation magnetization M_s is for Co^{2+} substituted Sr ferrite gives a value 28.33 emu/g.

REFERENCES

- [1] M. Jamalian, (2015). *Journal of Magnetism and Magnetic Materials*. 378, 217-220.
- [2] R.S. Azis, M. Hashim, N. Yahya, R. Alias, N.M. Saiden, N.A. Aini, A.A. Rejab, Z. Hari, (2002). in: *Proceedings Seminar Kimia Bersama: UKM-ITB Ke-5*, pp. 169.
- [3] J. Luo, Y. Xu, D. Gao, (2014). *Solid State Sciences*. 37, 40-46.
- [4] D. Wu, Z. Yang, F. Wei, M. Matsumoto, (2001). *Physica Status Solidi (a)*. 184, 157-163.
- [5] B.K. Rai, S.R. Mishra, V.V. Nguyen, J.P. Liu, (2013). *Journal of Alloys and Compounds*. 550, 198-203.
- [6] R.S. Azis, M. Hashim, N. Yahya, N.M. Saiden, Z. Hari, (2002). in: *Solid State Ionics. Trends in the New Millennium*, pp. 575-582.
- [7] M.N. Ashiq, M. Javed Iqbal, I. Hussain Gul, (2011). *Journal of Magnetism and Magnetic Materials*. 323, 259-263.
- [8] J. Muller, A. Collomb, (1992). *Journal of Magnetism and Magnetic Materials*. 103, 194-203.
- [9] K. Kimura, M. Ohgaki, K. Tanaka, H. Morikawa, F. Marumo, (1990). *Journal of Solid State Chemistry*. 87, 186-194.
- [10] C.M. Fang, F. Kools, R. Metselaar, G.d. With, R.A.d. Groot, (2003). *Journal of Physics: Condensed Matter*. 15, 6229.
- [11] I. Ali, M.U. Islam, M.S. Awan, M. Ahmad, M.N. Ashiq, S. Naseem, (2013). *Journal of Alloys and Compounds*. 550, 564-572.
- [12] F.S. Tehrani, V. Daadmehr, A. Rezakhani, R.H. Akbarnejad, S. Gholipour, (2012). *Journal of superconductivity and novel magnetism*. 25, 2443-2455.
- [13] A. Baniasadi, A. Ghasemi, A. Nematy, M. Azami Ghadikolaie, E. Paimozd, (2014). *Journal of Alloys and Compounds*. 583, 325-328.
- [14] H. Sözeri, H. Deligöz, H. Kavas, A. Baykal, (2014). *Ceramics International*. 40, 8645-8657.
- [15] Z.W. Li, Z.H. Yang, L.B. Kong, (2012). *Journal of Magnetism and Magnetic Materials*. 324, 2795-2799.
- [16] Y. Ebrahimi, A.A. Sabbagh Alvani, A.A. Sarabi, H. Sameie, R. Salimi, M. Sabbagh Alvani, S. Moosakhani, (2012). *Ceramics International*. 38, 3885-3892.
- [17] I. Ali, M.U.I. , M.S.A. , M.A. , M.N.A. , S.N., (2013). *Journal of Alloys and Compounds*. 550, 564-572.
- [18] M.J. Iqbal, M.N. Ashiq, (2008). *Chemical Engineering Journal*. 136, 383-389.